

Biometric Analysis of Human Ear Recognition Using Traditional Approach

Soumyajit Sarkar

April 13, 2016

Department of Electrical Engineering &
Computer Science

Abstract

Biometric ear authentication has received enormous popularity in recent years due to its uniqueness for each and every individual, even for identical twins. In this paper, two scale and rotation invariant feature detectors, SIFT and SURF, are adopted for recognition and authentication of ear images. An extensive analysis has been made on how these two descriptors work under certain real-life conditions; and a performance measure has been given. The proposed technique is evaluated and compared with other approaches on two data sets. Extensive experimental study demonstrates the effectiveness of the proposed strategy. Robust Estimation algorithm has been implemented to remove several false matches and improved results have been provided. Deep Learning has become a new way to detect features in objects and is also used extensively for recognition purposes. Sophisticated deep learning techniques like Convolutional Neural Networks(CNNs) have also been implemented and analysis has been done. Deep Learning Models need a lot of data to give a good result, unfortunately ear datasets available publicly are not very large and thus CNN simulations are being carried out on other state of the art datasets related to this research for evaluation of the model.

Contents

Abstract	i	
1	Introduction	1
2	Statement of the Problem	6
2.1	Types of Biometrics	6
2.2	Purpose of Biometric Ear Recognition	7
2.3	Contributions of this Project	10
3	Background and Related Works	11
4	Traditional Design	15
4.1	Traditional Approach	15
4.2	SIFT and SURF Descriptor	17
4.3	False Match Removal	21
4.4	Training Model	24
4.5	Results of the Traditional Approach	28
5	Ongoing and Future Work	31
5.1	Deep Learning Approach	31
5.2	Convolutional Neural Networks	37
6	Conclusion	41
	Bibliography	43
7	Appendix	50

List of Figures

1.1	The pipeline of the proposed Ear Recognition System	3
2.1	Characteristics of Human Ear [1]	8
4.1	Ear Image Enhancement	15
4.2	Histogram of Enhanced Image	16
4.3	Number of Features Detected	16
4.4	The detected SURF features (left) and matching result under rotation (middle) and scale change (right)	19
4.5	The matching results of SIFT detectors under rotation (left) and scale change (right)	21
4.6	Feature Point Matches after Outlier Detection	24
4.7	The matching results of SURF detector	25
4.8	The matching results of SIFT detector	26
4.9	Multi-class SVM(from [2])	26
4.10	A comparison result of the detected and matched keypoints by SURF and SIFT	30
4.11	Sample Images from IIT Delhi Ear Dataset	30
4.12	Sample Images from AMI Ear Dataset	30
5.1	Artificial Neural Network with D input neurons and 1 output neuron	32
5.2	LeNet Network Diagram	37
5.3	Typical CNN Network	37
5.4	Performance of a 4-layer ReLU CNN	39

List of Tables

4.1	SIFT and SURF detection and matching results at different scales	29
4.2	Experimental results on the IIT Delhi database	29
4.3	Einal Results after the outlier detection	29

Chapter 1

Introduction

Biometric authentication of people based on various anatomical characteristics, like eye, ear, face, iris, and fingerprint have attracted lots of attention during the past few decades, and some of these techniques have already been successfully applied for recognition and authentication. However, many systems are not very robust and may fail to work under certain conditions. Biometric ear recognition is a relatively new technique that may surpass the existing systems due to several significant reasons. For example, the acquisition of ear images is relatively easy and, unlike iris, can be captured without the co-operation of individuals [1]

Human ear contains rich and stable features which are more reliable than face features, as the structure of the ear is not subject to change with age. It has also been found out that no two ears are exactly the same even for identical twins [3]. The detailed structure of ear is not only very unique but also permanent, since the shape of a human ear never shows drastic changes over the course of life. The research on ear identification was first conducted by Bertillon, a French criminologist, in 1890. The process was refined by American police officer, Iannarelli [20], who divided the ear based on various distinctive features of seven parts: i.e. helix,

concha, antihelix, crux of helix, inter- tragic notch, tragus, and antitragus [4].

One of the first ear recognition systems is Iannarelli's system developed originally in 1949. This manual system has basically 12 measurements. Each photograph of the ear is aligned such that the lower tip of a standardized vertical guide on the development easel touches the upper flesh line of the cocha area, while the upper tip touches the outline of the antitragus. Then the crux of helix is detected and used as a center point. Vertical, horizontal, diagonal, and anti-diagonal lines are drawn from that center point to intersect the internal and external curves on the surface of the pinna. The 12 measurements are derived from these intersections and used to represent the ear [3].

Fields et al. [1960] made an attempt to identify newborn babies in hospitals. They visually assessed 206 sets of ear photographs, and concluded that the morphological constancy of the ear can be used to establish the identity of the newborn.

The human ear starts to develop between the fifth and seventh weeks of pregnancy. At this stage, the embryos face takes on more definition as a mouth perforation, nostrils, and ear indentations become visible. Though there is still disagreement as to the precise embryology of the external ear , the ear development during pregnancy is listed below:

- 1) The embryo develops initial clusters of embryonic cells that serve as the foundation from which a body part or organ develops. Two of these clusters, termed the first and second pharyngeal arches, form six tissue elevations called auricular hillocks during the fifth week of development.
- 2) In the seventh week, the auricular hillocks begin to enlarge, differentiate, and fuse, producing the final shape of the ear, which is gradually translocated from

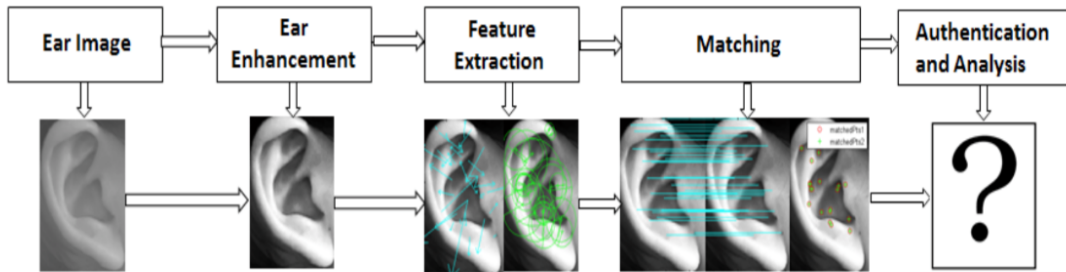


Figure 1.1. The pipeline of the proposed Ear Recognition System

the side of the neck to a more cranial and lateral site. By the ninth week, the morphology of the hillocks is recognizable as a human ear.

Currently there is no such biometric system which is being used commercially for automatic identification or verification of the ear biometric.

Here, we propose to use two scale and rotation invariant feature detectors, i.e. SIFT (scale invariant feature transform) and SURF (speed up robust features), for ear recognition. Both SIFT and SURF extract specific interest points from an image and generate descriptors for the feature points to form a reliable matching results.

Extensive experiments have been carried out on two different sets of databases to evaluate their performance with respect to various rotations and scales. One of the most important feature of ear images is its easiness in acquisition, however, the acquired images may be in different scales, rotations, and illumination. The scale and rotation invariant property of the SIFT and SURF algorithms makes them perfect for ear authentication under various circumstances.

A new concept in the field of machine learning and computer vision has come up which has surpassed the traditional object recognition methods. This new approach is called deep learning. Deep Learning is a branch of Machine Learning

which has multiple levels of representations and abstractions. It is basically a rebranding of the term Artificial Neural Networks. Deep Learning algorithms have already been applied in Apple's Siri, Google's Streetview etc.

The reason behind the rise of ear biometrics is that the structure of the ear is not only unique but also permanent. Since the acquisition of ear images does not require a person's co-operation, due to these advantages the interest in ear recognition research has grown significantly in the past few years. One of the most important challenges in ear biometrics is occlusion and pose variation, in contrast to the face, the ear is sometimes partially occluded by hair, ear-rings, headphones. Robustness against occlusions have been addressed in previous publications [1]. But no studies have been covered on the effect of certain types of occlusion like hair or earrings.

Pose variations has also been another challenge in this domain where the subject's ear is never straight and is moving all the time when the images are captured from different angles. Thus scalability and pose remains a concern. In this project, details on pose variations and scales have been provided and analysis has also been done to see how it affects the performance of the system.

The symmetry of the right and left ear has not been understood yet. The studies of Iannarelli indicates that some characteristics of the outer ear can be inherited and another factor is ageing. These assumptions does not have a proof since ear recognition is still a relatively new field of research. Lighting conditions, pose variations till remain a great challenge to the performance of the biometric systems. Though good databases are available, it is still difficult to get better performances as most of the databases follow a specific standard and they are taken under the same light and pose variations.

The rest is organized as follows. Some background and related research are discussed in Section 3; The proposed method is presented in details in Section 4; Some experimental results and analysis are given in Section 4.5; Ongoing and future work is being described in Section 5 with Conclusion in Section 6.

Chapter 2

Statement of the Problem

2.1 Types of Biometrics

Biometrics has been an active field of research over the last decade. The reason behind their success is that biometric characteristics are universal, unique and permanent. Unlike other forms of authentication such as passwords or identification cards which can be stolen or faked easily.

There are many kinds of biometrics which can be used for authentication purposes. Among them the prominent being, Face, Ear, Palm, Fingerprint [5], Iris and others which are frequently being used these days in day to day life to authenticate an individual. Another reason biometrics have been used these days are due to terrorist activities and other fraudulent ways in which people impersonate themselves which are harder to catch. These days biometrics are used everywhere from Airports to ATMs to secured entry to corporate offices where checking the identity of an identity of an individual is mandatory before access is given. It helps to strengthen the security of an organization or country potential threat. As mentioned above, the different types of biometrics, different biometrics

have different purposes and importance. The most popular being face recognition which is being used everywhere to authenticate people, the only disadvantage being the change in facial expression and with age the face changes upto a certain extent which makes it difficult to recognize and authenticate. Fingerprint is also being used in almost any high priority zone nowadays to authenticate and is very successful but it requires complete co-operation of an individual in order to authenticate them. The same problem happens with iris authentication where it becomes very difficult to extract the iris image to match and authenticate.

Ear authentication comes to the rescue in such a situation due to many reasons. The primary being the stability in the human ear structure and ear images can easily be captured without the co-operation of an individual. Each ear is unique, so any side image of an individual is enough in order to authenticate a person.

2.2 Purpose of Biometric Ear Recognition

Ear authentication and recognition is being considered as one of the most innovative processes as of today. The human ear can be divided into six main parts: Outer helix, the antihelix, the lobe, the tragus, the antitragus and the concha. The shape of the outer ear evolves during the embryonic state from six growth nodules. The structure is completely random, the randomness can be observed by comparing the left and right ear of the same person - thus they are not symmetric. French criminologist Alphonse Bertillon was the first to be aware of ear to be used for human identification purposes. His work was carried on by Alfred Ianarelli who collected 10,000 ear images and determined 12 characteristics needed to identify a person. He also conducted studies on twins and triplets thereby discovering that ears are unique even among genetically identical persons

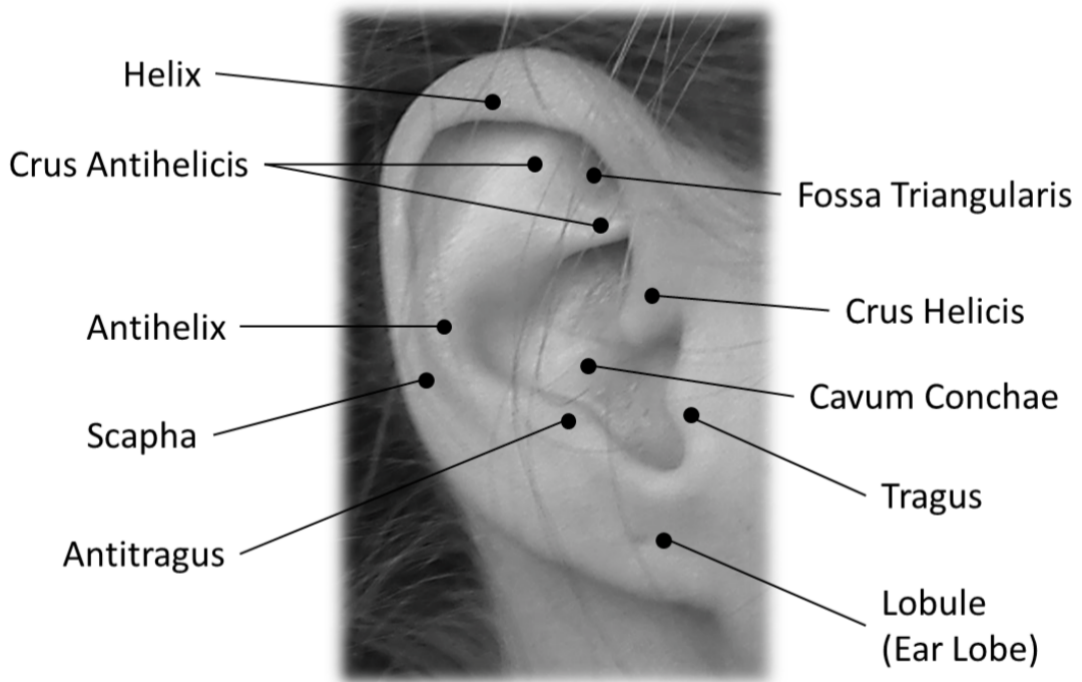


Figure 2.1. Characteristics of Human Ear [1]

[1]. The different parts of the ear are shown in Figure 2.1

The uniqueness of the ear has been accepted to be true based on empirical results, the underlying scientific basis of ear individuality has not been formally established. As a result, the validity of ear evidences has been challenged in several court cases. In response to a U.S Court Ruling, a large scale study involving 10,000 subjects has been proposed to determine the variability of the ear from the entire dataset. In 1906, Imhofer studied a set of 500 ears and noted that based on 4 features - he could clearly distinguish between ears. In 1989, Iannarelli [6] examined the difference in ear structures between fraternal and identical twins, it was found that despite having the same ear structures, they were still clearly distinguishable.

In 2000, Burge and Burger [7] presented a study of the uniqueness of human

ear by using Iannarelli's features, they assumed an average standard deviation in the population of 4 units, the 12 measurements provided a space with 4^{12} variation which is less than 17 million distinct points. Purkait and Singh [8] in 2008, presented a preliminary study to test the individuality of human ear patterns. They manually extracted 12 inter-landmark linear distances from a set of 700 male and female individuals. They found that this 12-dimensional feature space could clearly distinguish more than 99.9% of ear pairs, where very few pairs had distances which fell below the safe distinction limit.

The typical ear biometric system can be viewed as a system where an input image can be reduced to a set of features that is used to compare with the features of other images to determine its identity. The salient features of a classical ear recognition system are [3]

1. Ear Detection/ Segmentation - The first stage which is used to localize the position of the ear in the image.
2. Ear Normalization and Enhancement - The size of the ear image is normalized for standardization and enhanced using standard image processing techniques in order for more features to be extracted.
3. Feature Extraction - Feature extraction refers to a process in which the ear image is being reduced to a mathematical model called a feature vector to get information.
4. Matching Features - The features extracted are then compared to the features that are extracted earlier and stored in the database to find a match.
5. Decision - Matching scores are generated by the model used to train the features to give a decision of whether the image is matched or not.

2.3 Contributions of this Project

The main goal of this work is to develop shallow and deep techniques to extract efficient features from a set of ear images in order to authenticate a human being. A thorough comparison of two traditional techniques called SIFT(Scale-Invariant Feature Transform) [9] [10] and SURF(Speed-up of Robust Features have been provided) [11], this project is a continuation of the work done by Sarkar et al [12]. Since the extracted features are hand-crafted, there is quite a good amount of false matching and thus it may affect the true performance of the whole process. Outlier detection is a way in Computer Vision by which several false matches can be eliminated in order to get a proper result.

Chapter 3

Background and Related Works

Human ears start to develop between fifth and seventh weeks of pregnancy. At this stage, the embryo face takes on more definition as mouth perforation, nostrils and ear indentations become visible. Forensic science literature reports that ear growth after the first four months of birth is highly linear [6]. The rate of stretching is five times greater than normal during the period from 4 months to the age of 8, after which, it is constant until the age of seventy when it again increases. Thus it can be said that ear remains almost unchanged during a substantial period of 62 years and, thus, it is one of the strong points of considering ear for biometric authentication.

In early approaches to ear detection, several edge detection algorithms like Canny [13], Harris corner detectors [14] were used to segment the ear images from the background, but now more sophisticated approaches have come up.

Haar-based methods have given fairly better results for face detection as it is robust and fast. The different types of ear recognition systems include those of intensity-based, force-field based, 2D curves geometry, wavelet transformation, Gabor filters, SIFT, and 3D features. The force-field transforms gained popu-

larity due to its uniqueness and efficiency [15]. Similar methods have also been implemented on other kinds of ear recognition systems [16] [17].

Deep Methods have already come up and showing good performances on other face recognition systems which shows that it can also be applied to ear recognition systems. Hand-crafted feature detectors have not been able to work properly and are not robust, so deep features have been extracted to improve upon the performance. But one of the few drawbacks about deep learning is that it needs a large amount of data to train the model. There are not many ear databases that are too big but an attempt has been made to apply deep learning on a small scale database and analyze the results.

The goal of this project is to build deep learning models that can be robust and can be applied to all sorts of recognition processes. In traditional methods, the result did not depend on the size of the dataset as the features are extracted individually and no layers are being formed as the network was shallow, but deep learning models need a lot of data to process and as a matter of fact, a lot of data is needed to extract the individual features from the respective images. One of the primary reasons behind Deep Learning models failing in the last decade was that there was not enough data to train the deep learning models. The availability of vast amount of data in every domain ranging from images to raw data has made it possible for deep learning systems to give better performances.

Another reason deep learning algorithms were not being able to perform properly was that of computation ability of CPUs, the advent of modern GPUs have made the training process even faster. Companies like NVIDIA and others have been in the forefront to provide GPUs for research and commercial purposes. Training time has been decreased significantly even after processing millions of

images. Thus with the help of great deep learning frameworks like CAFFE [18], Theano [19], Torch [20] , NVIDIA GPU [21] Digits, Google TensorFlow [22] and their combination with GPUs , training has been made faster and thus more and more methods can be applied. Various research institutions and commercial companies have been using deep learning since the last decade and getting tremendous success in object recognition, object classification, image retrieval, image classification, speech recognition, object recognition, biometrics, data analytics, machine learning and many other techniques.

It has also been seen that one deep learning model can be used for a variety of tasks ranging from working with raw data to images to speech data etc. Thus it makes it easier to create one model and use everywhere unlike the shallow techniques which had to be specifically hand-crafted for specific purposes and thus imposed a great problem for researchers. Currently, researchers are working on the disadvantages that deep learning has which is, the model needs a lot of data to be trained but humans can recognize themselves with very few training data and that is why research is going in this field to eliminate this barrier so that deep learning techniques will be able to learn from a small dataset and give equally good performances that they are producing on a model trained with a large dataset.

A lot of work has been happening in the ear biometrics over the past decade. The approaches are varied with some working on Intensity-based features while others on 2-D ad 3-D curves etc. Chang et al.[2003] whole worked on the UND database and got an accuracy of 72.7% using the PCA [23] approach. A new concept called Force-Field was being brought by Hurley [15] et al. which gave an accuracy of 99.2 % on the XM2VTS dataset. Many other approaches like

3D Features, Gabor Filters, SIFT, Wavelet Transformation have been applied on different databases and results have been obtained. This project is mostly on the analysis of Biometric Human Ear datasets on two methods - SIFT and SURF and a comparison is given on the rotation and scaling factors and how the number of features varies on such conditions keeping the real life scenarios in mind where Ear images are not obtained as compared to a dataset.

Similar methods have been applied on other Biometrics like face, fingerprint and others etc. Both Shallow and Deep methods have different significances. Shallow methods start by extracting a representation of the image using hand-crafted local image descriptors like SIFT, SURF ,LBP,HoG [24–27] then the local features are being aggregated into an overall ace descriptor by using a pooling mechanism for example Fisher Vector [28] [29]. The work of deep learning was initiated with the help of a CNN Feature Extractor , a learnable function obtained by composing several linear and non-linear operators. The best example can be shown in DeepFace [30] which uses deep CNN trained to classify faces using a dataset of 4 million examples spanning 4000 unique identities. Upon extensive research, new ideas were being incorporated using multiple CNNs [29].

Chapter 4

Traditional Design

4.1 Traditional Approach

Real-life ear images can be acquired in various formats with different scaling and rotation conditions. In this paper, we propose to use scale and rotation invariant feature detectors to describe interested features and match them with other images in the databases. The proposed ear recognition technique is shown in Figure 1.1. Below is a brief description of each function block.



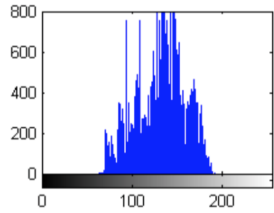
(a) Original Ear Image



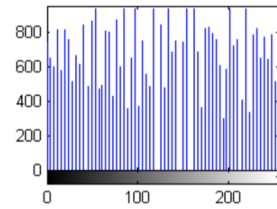
(b) Enhanced Ear image

Figure 4.1. Ear Image Enhancement

The ear enhancement process starts with contrast enhancement, where we apply histogram equalization to improve the contrast in an image in order to

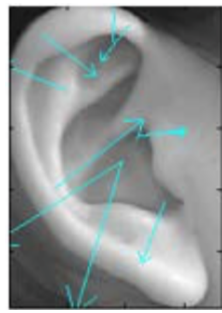


(a) Histogram of Original Image

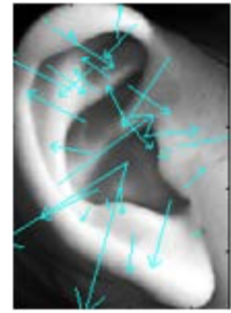


(b) Histogram of Enhanced Image

Figure 4.2. Histogram of Enhanced Image



(a) 10 SIFT features detected in the original image



(b) 32 SIFT features detected in the original image

Figure 4.3. Number of Features Detected

stretch out its intensity range, from which, we get an enhanced version of the original image by maximizing the contrast level of an image, as shown in Figure 4.1

Feature Extraction is the process of extracting salient features from the image, and each feature is described by a vector which summarizes the required information for that point [2]. Features are extracted exclusively in order for the image to be matched with the features of the input image to authenticate the ear so that a decision can be made. In this paper, two rotation and scale invariant features are studied. The details are being discussed in the next section.

4.2 SIFT and SURF Descriptor

Speed up Robust Features(SURF) - SURF is a high performance, fast scale and rotation invariant point detector and descriptor. The task of finding point correspondences between two images of the same scene or object is part of many computer vision applications. Image registration, camera calibration, object recognition, and image retrieval are just a few. The search for discrete image point correspondences can be divided into three main steps. First, interest points are selected at distinctive locations in the image, such as corners, blobs, and T-junctions. The most valuable property of an interest point detector is its repeatability. The repeatability expresses the reliability of a detector for finding the same physical interest points under different viewing conditions. Next, the neighbourhood of every interest point is represented by a feature vector. This descriptor has to be distinctive and at the same time robust to noise, detection displacements and geometric and photometric deformations. Finally, the descriptor vectors are matched between different images. The matching is based on a distance between the vectors, e.g. the Mahalanobis or Euclidean distance. The dimension of the descriptor has a direct impact on the time this takes, and less dimensions are desirable for fast interest point matching. However, lower dimensional feature vectors are in general less distinctive than their high-dimensional counterparts. It has been our goal to develop both a detector and descriptor that, in comparison to the state-of-the-art, are fast to compute while not sacrificing performance. In order to succeed, one has to strike a balance between the above requirements like simplifying the detection scheme while keeping it accurate, and reducing the descriptors size while keeping it sufficiently distinctive. It outperforms previously proposed schemes with respect to repeatability, distinctiveness

and robustness [9]. The detector is based on the Hessian matrix and uses a very basic Laplacian-based detector, called difference of Gaussian (DoG). The implementation of SURF can be divided into three main steps. First, interest points are selected at distinctive locations in the image, such as corners, blobs, and T-junctions. Then, the neighborhood of every interest point is represented by a feature vector. This descriptor has to be distinctive and robust to noise, detection errors, and geometric and photometric deformations. Finally, the descriptor vectors are matched between different images. When working with local features, the issue that needs to be settled is the required level of invariance. Here the rotation and scale invariant descriptors seem to offer a good compromise between feature complexity and robustness to commonly occurring deformations, skew, anisotropic scaling, and perspective effects [9].

Given a point in an Image, the Hessian matrix is as follows:

$$H(x, \sigma) = \begin{bmatrix} L_{xx}(x, \sigma) & L_{xy}(x, \sigma) \\ L_{xy}(x, \sigma) & L_{yy}(x, \sigma) \end{bmatrix}$$

where $L_{xx}(x, \sigma)$ is the convolution of the gaussian second order derivative $\frac{d^2}{dy^2}g(\sigma)$ at the point. This method leads to a novel detection, description and subsequent matching steps. Using relative strengths and orientations of gradient reduces the effect of photometric changes. Figure 4.4 shows the detection results with respect to rotation and scale change. As shown in Section 4, it has been found that though SURF is rotation invariant, its performance in matching, i.e. matching score, decreases sharply when the images are rotated or scaled. The SURF features are not stable over various rotation angles and scale changes.

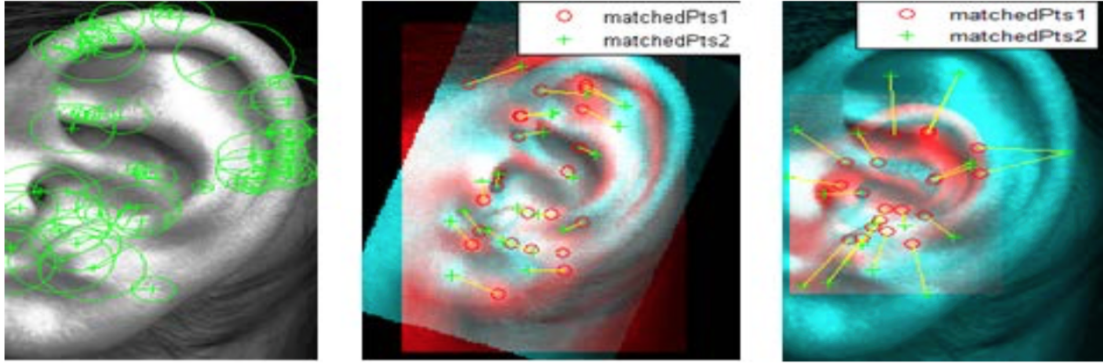


Figure 4.4. The detected SURF features (left) and matching result under rotation (middle) and scale change (right)

Scale Invariant Feature Transform(SIFT) - The SIFT features are invariant to image scaling and rotation and shown to provide robust matching across a substantial range of affine distortion, change in 3D viewpoint, addition of noise, and change in illumination. Image matching is a fundamental aspect of many problems in computer vision, including object or scene recognition, solving for 3D structure from multiple images, stereo correspondence, and motion tracking. This paper describes image features that have many properties that make them suitable for matching differing images of an object or scene. The features are invariant to image scaling and rotation, and partially invariant to change in illumination and 3D camera viewpoint. They are well localized in both the spatial and frequency domains, reducing the probability of disruption by occlusion, clutter, or noise. Large numbers of features can be extracted from typical images with efficient algorithms. In addition, the features are highly distinctive, which allows a single feature to be correctly matched with high probability against a large database of features, providing a basis for object and scene recognition. The cost of extracting these features is minimized by taking a cascade filtering approach, in which the more expensive operations are applied only at locations that pass an initial

test. 3D-SIFT [31] algorithms have also been researched upon to get a better understanding for 3-dimensional object feature extraction and matching.

The computation stages of SIFT are as follows:

Step 1. Scale space extrema detection: The first step is to construct a Gaussian scale over all the locations. It is implemented efficiently by using a difference of Gaussian (DoG) to identify potential interest points. The 2D Gaussian operator $G(x,y,\sigma)$ is convolved with the input image $I(x,y)$:

$$L(x, y, \sigma) = G(x, y, \sigma) * I(x, y)$$

where the DoG images are obtained by subtracting the subsequent scales in each octave.

$$G(x, y, \sigma) = L(x, y, k\sigma) - L(x, y, \sigma)$$

Step 2. Accurate keypoint localization: Once a keypoint has been detected, a detailed model is fitted to determine its location and scale. The keypoints are selected based on measures of their stability. Further details can be found in [32].

Step 3. Orientation assignment: One or more orientations are assigned to each key- point location based on local image gradient directions. All future operations are per- formed on image data that has been transformed relative to the assigned orientation, scale, and location for each feature.

Step 4. Keypoint descriptor: The local image gradients are measured at se- lected scale in the region around each keypoint. They are transformed into a certain representation that allows for significant levels of local shape distortion and shape illumination.

Figure 4.5 shows an evaluation of the SIFT detector. It is evident the SIFT keypoints are very stable when the images are rotated and scaled. The scaling results are much better compared to the rotation results in our experiments.



Figure 4.5. The matching results of SIFT detectors under rotation (left) and scale change (right)

4.3 False Match Removal

Fundamental Matrix estimation from two views plays an important role in 3D Computer Vision. It contains all geometric information about the relative transformation between images. The estimation is actually based on solving a homogeneous linear system where each linear equation is formed by a pair of correspondence feature points. A large number of robust estimation approaches have been proposed to alleviate the influence of outliers to the fundamental matrix estimation. Some of them include the M-estimator method which reduces the effect of outliers by applying weight functions to transform the problem to a weighted least squares problem. However, the approach needs a good initial estimation and only works under low percentages of outliers. This method is very time-consuming.

Random Sample Consensus or RANSAC [33] [34] is a very popular algorithm for Fundamental Matrix Estimation. It uses minimal points set to estimate an initial guess and then the confidence of the estimation is established by testing each point correspondence against the model with an inlier set, which is determined by choosing points that have error below a given threshold. After that, a new fundamental matrix is estimated by the inlier set, thus iteratively the RANSAC

algorithm attempts to find a solution that maximizes the amount of inlier set.

Re-projection error is adopted in this approach [35] rather than the widely used algebraic error for confidence evaluation purposes. An assumption is made of gaussian noise present in each image and the reprojection error of point correspondence can be described by a chi-square distribution. The outliers are eliminated by a 3-sigma principle.

For Robust Fundamental Matrix Estimation, an Eight-point linear algorithm is used, where estimation from a set of point correspondences between two images is performed. Given a set of two images I and I' , suppose $x_i \in I$ and $x'_i \in I'$ are a pair of corresponding homogeneous points between the two images, The fundamental matrix \mathbf{F} satisfies the following equation:

$$x_i'^T \mathbf{F} x_i = 0$$

where the fundamental matrix is a 3 X 3 homogeneous matrix defined up to scale. Each pair of point correspondence yield one linear constraint for the entries of \mathbf{F} . Thus the estimation of the fundamental matrix can be done with eight point pairs. When more correspondences are available, the fundamental matrix can be estimated via least squares.

To evaluate the error for each pair of point correspondence, a perspective 3D reprojection of all the corresponding points can be obtained via triangulations. The reconstructed 3D points can be reprojected back to the two images via the camera matrices. let us suppose $\hat{\mathbf{x}}_i$ and $\hat{\mathbf{x}}'_i$ are the reprojected images of point i , the 2D reprojection error of the corresponding point is defined as

$$e_r(i) = \frac{1}{2} \sum \| \mathbf{x}_i - \hat{\mathbf{x}}_i \|^2_F + \| \mathbf{x}'_i - \hat{\mathbf{x}}'^2_i \|^2_F, \quad s.t. \quad \hat{\mathbf{x}}_i'^T \mathbf{F} \hat{\mathbf{x}}_i = 0 \quad \forall i \quad (4.1)$$

The 2D reprojection error is proven to be more superior to other geometric errors. Optimal triangulation is a linear triangulation method which converts the least-square function to a one parameter function and finds a global optimal solution.

Now, for the strategy for outlier detection, it is being assumed that the image noise is modeled by Gaussian distribution. Through intensive simulations, it is being found that the reprojection errors of outliers are usually greatly larger than those of inliers. As a result, these outliers can be identified using 3-sigma principle. Points with reprojection errors larger than the triple variance of all the reprojection error can be classified as outliers. Based on robust statistics [15:Ming Paper], we can obtain a robust standard deviation of the reprojection errors by the following equation.

$$\sigma = 1.4826 \left(1 + \frac{5}{n - q} \right) \text{median}_i |e_i^r| \quad (4.2)$$

The above equation is the median absolute deviation (MAD) scale estimate. The first number is obtained from the inverse of the cumulative normal distribution, and the term $(1 + 5)$ is the finite sample correction factor with the total number of nq parameters $q = 8$ and n the total number of features. According to the distribution model, we distinguish the inliers from their reprojection errors of each pair of corresponding points. The points whose reprojection errors are less than 3σ are deemed as inliers, since 99.14% of the data points lies within 3σ under the assumption of the Gaussian distribution error model.

The Fast and Robust Algorithm is as follows:

1. Normalize the coordinates of all matching points;
2. Estimate an initial fundamental matrix using eight-point linear algorithm;

3. Compute the reprojection error and determine an outlier threshold;
4. Re-estimate the fundamental matrix using the inliers detected in step 3;
5. Repeat the steps 3 and 4 one time to refine the inlier set;
6. Estimate the optimal fundamental matrix using the inliers obtained in step 5.

After simulations are being carried out, it has been seen that the number of matching keypoints decreases after the outlier detection. As shown in Figure 4.6, the number of keypoints obtained by SIFT was 27, but after False Matches are removed via the 3σ principle, the number of proper matches come down to 22. Thus making the algorithm more robust to false matches.

4.4 Training Model

Machine Learning models have previously worked wonders on the correct recognition of various algorithms when features extracted are fed into the model for it to figure out the false and the true cases.

Support Vector Machines(SVMs) [36] brought a completely new idea to the

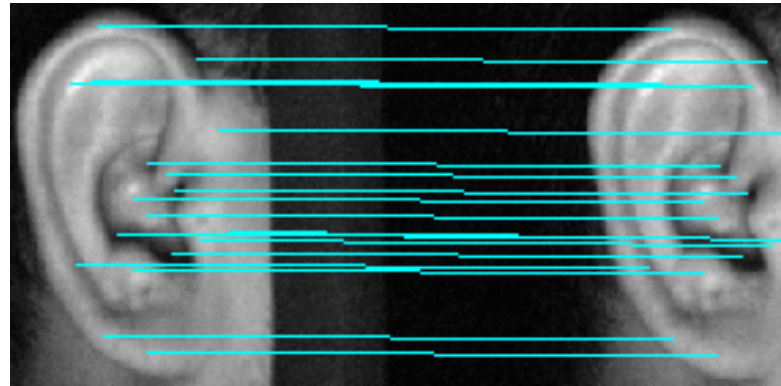


Figure 4.6. Feature Point Matches after Outlier Detection



Figure 4.7. The matching results of SURF detector

field of machine learning. SVMs were introduced in COLT-92 by Boser, Guyon and Vapnik. For Pattern Recognition, SVMs have been used for Handwriting Recognition, Object Recognition, speaker identification, charmed quark detection, text categorization, face detection in images and many other purposes. SVMs are supervised learning models, with learning algorithms which are associated with it which are used to analyze data for classification and regression purposes. Given a set of training examples, each marked for belonging to one of two categories, an SVM training algorithm builds a model that assigns new examples into one category or the other, making it a non-probabilistic binary linear classifier. An SVM model is a representation of the examples as points in space, mapped so that the examples of the separate categories are divided by a clear gap that is as wide

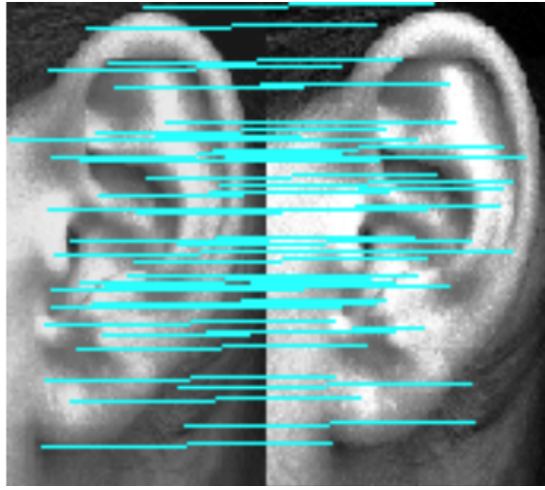


Figure 4.8. The matching results of SIFT detector

as possible. New examples are then mapped into that same space and predicted to belong to a category based on which side of the gap they fall on.

In addition to performing linear classification, SVMs can efficiently perform a non-linear classification using what is called the kernel trick, implicitly mapping their inputs into high-dimensional feature spaces. When data are not labeled, a supervised learning is not possible, and an unsupervised learning is required, that

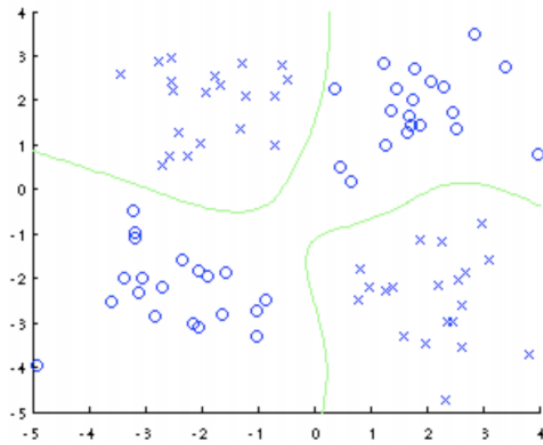


Figure 4.9. Multi-class SVM(from [2])

would find natural clustering of the data to groups, and map new data to these formed groups. The clustering algorithm which provides an improvement to the support vector machines is called support vector clustering and is often used in industrial applications either when data is not labeled or when only some data is labeled as a preprocessing for a classification pass.

SVMs can be divided into linear SVM and multi-class SVM, here we are more concerned with multiclass SVM [37].

For our purpose we have used Multi-class SVMs. Support Vector Machines were originally designed for binary classification. The formulation to solve Multi-class SVM must have variables which are proportional to the number of different classes. The concept of SVM was proposed by Vapnik et al. They helped to classify almost everything right from linear problems to multi-dimensional problems where the kernel matrix is used to transform the conflicting points into a different dimensional space called the kernel space in order to draw a hyperplane in a conclusive manner so as to separate the different cases. Here multiclass SVM is being used in order to classify the features as extracted by the various feature extraction techniques like SURF and SIFT. After that the model is trained and the features are matched with the features obtained from the query ear image in order to find a nearest match to succeed. Since it is multi-class, thus it helps to create separate classes for different classes of images and helps to classify them when the matching process is being done. The main process of better classification of the model depends on the input features. So as a matter of fact we can say that better the feature extraction is being done, better will be the classification made by the multiclass SVM and thus better will be the results.

4.5 Results of the Traditional Approach

The proposed approach has been evaluated on two data sets. One is the AMI database [38], which consists of 175 ear images; and the other is the IIT Delhi database [39], which consists of 494 images of 125 distinct persons. The images were all converted to gray- scale images for ease of work. It has also been found out that contrast enhancement is an important factor for feature detection and matching, because it makes the feature detectors find better set of keypoints and increase the effectiveness of matching. According to the experiments performed, it has been found that upper helix, antihe- lix, and tragus are the most important regions for feature selection compared to others. These regions contribute to about 64% of the feature points. Figure 7 shows some sample images from the two databases we used for our exper- iments. The graphs in Figure 8 indicates the average number of keypoints found and matched by SIFT and SURF detectors when the images are rotated from a range of 0 to 180 degrees. The results suggest that the SIFT detector is fairly stable over a variation of angles from 20 to 160 degrees, whereas the SURF detector, though faster and rotation invariant, is not very stable. Table 1 shows the keypoints detected and matched by the SIFT and SURF detectors, where the performance ratio is the ratio of the number of matched points to that of detected features. It is obvious that the SIFT algorithm performs better when the sizes of images are decreased, while the SURF algorithm performs better when the image sizes are increased. However, the amount of detected keypoints by the SIFT detector is always higher than that by the SURF detector.

Table 2 shows an overview of how the two detectors work in real-life conditions where some images are not matched due to illumination changes as those images

Table 4.1. SIFT and SURF detection and matching results at different scales

Scaling	Methods	0.25	0.5	0.75	1.0	2.0	3.0	4.0
Number of Features	SIFT	28	53	58	64	170	247	233
	SURF	3	12	30	41	39	41	44
Number of Matches	SIFT	24	45	54	64	53	47	51
	SURF	2	9	23	41	20	21	16
Performance Ratio	SIFT	0.85	.85	0.89	1.0	0.32	.20	0.22
	SURF	0.67	0.75	0.75	1.0	0.51	0.51	.30

Table 4.2. Experimental results on the IIT Delhi database

Method	Number of Images	Matched	Unmatched	Time	Recognition Rate
SIFT	125	121	4	0.21	96.8 %
SURF	125	118	7	0.183	94.4 %

were mostly taken at night and at different angles. Thus, the descriptors fail to find enough feature keypoints for matching. The overall recognition rates of the SIFT and SURF algorithms on the IIT Delhi database are 96.8% and 94.4%, respectively. As a comparison, we also implemented other methods for ear recognition. The template matching technique yields a recognition rate of 93 % for [40], and 92.6 % for [41], whereas the recognition rate by the contour extraction technique [42] is 85 %. It is evident that the proposed technique yields a higher recognition rate.

Table 4.3. Final Results after the outlier detection

Method	Number of Images	Matched	Unmatched	Recognition Rate
SIFT	125	119	6	95.2 %
SURF	125	114	11	91.2 %

From the above table 4.3, it can be seen that due to the removal of outliers - the number of false matches have decreased to a certain extent. Thus, the false matches have been successfully removed keeping in mind that the noise in the image is gaussian, the performance of the algorithm decreases but the algorithm is robust and thus is more favourable than the previous approach.

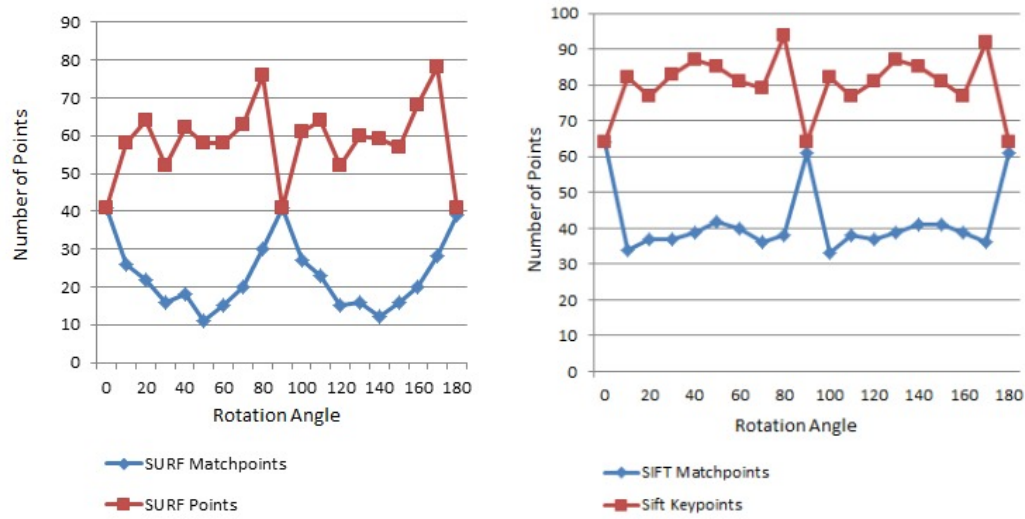


Figure 4.10. A comparison result of the detected and matched keypoints by SURF and SIFT

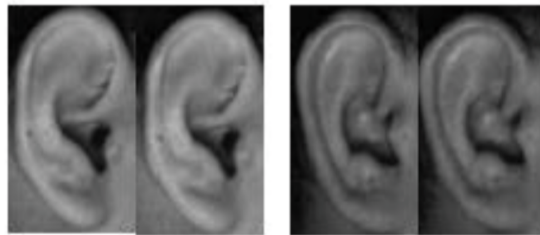


Figure 4.11. Sample Images from IIT Delhi Ear Dataset



Figure 4.12. Sample Images from AMI Ear Dataset

Chapter 5

Ongoing and Future Work

5.1 Deep Learning Approach

Artificial Neural Networks [43] shown in Figure 5.1 was an idea conceived in the 1960s to mimic the functions of the human brain in the way it absorbs information and learns from it. In order to convert the whole notion into reality it took a lot more time than expected. The primary reason behind the delay is that back then, the computers were not powerful enough, the other reasons being the researchers were not totally aware of the problem. Then in 1986, eminent neural network researcher and computer scientist Dr. Geoffrey Hinton came up with the idea of backpropagation [44] where a Deep Neural Network could be trained discriminatively and the weight updates can be done via stochastic gradient descent using the following equation.

$$w_{ij}(t+1) = w_{ij}(t) + \eta \frac{\partial C}{\partial w_{ij}}$$

where η is the learning rate, C is the cost function. The choice of the cost function depends on factors such as learning type whether it be supervised, unsupervised

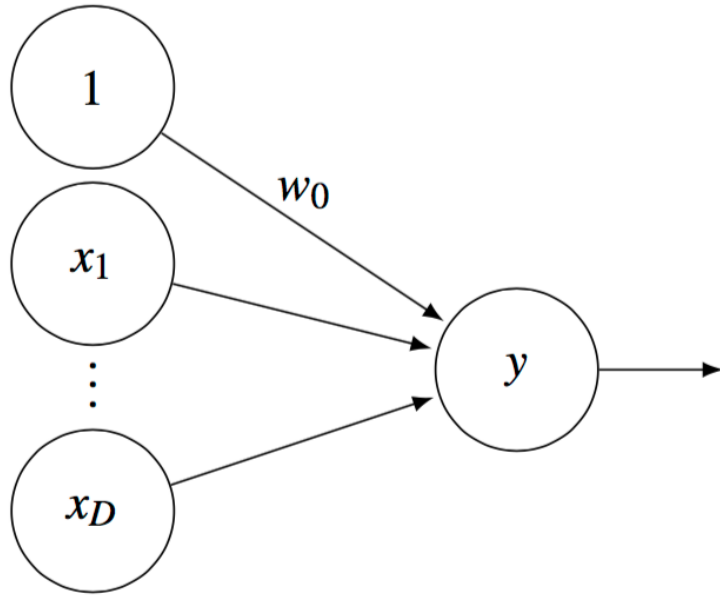


Figure 5.1. Artificial Neural Network with D input neurons and 1 output neuron

or reinforcement learning.

The ability of multi-layer backpropagation networks has enabled the machines to learn complex high-dimensional non-linear mappings from large collections of example data which makes it obvious for visual recognition. In this method, rather than hand-crafting the various features, a raw image is first convoluted with a filter to find various feature maps. The feature maps are then connected together to form a fully-connected layer, the input of one layer is fed as the output of the next layer to create a deep network. The whole process rely on backpropagation to turn the first few layers into an appropriate feature extractor. Deep learning has achieved a lot of successes in the past for character recognition, digit recognition and recent works show that it is being applied to most topics of image representation and learning purposes. Just recently it has been applied to Face Recognition by training with lots of face image data and tremendous success

has been reported[deep face paper].

The whole process of deep Convolutional Neural Networks(CNN) [45] is very complex and requires a lot of computation to train and as a matter of fact, parallel computing is being brought forward to decrease the training time. The fully connected layer has several hundred hidden units and each of these units have specific weights assigned to them with the help of the back-propagation algorithm. Overfitting occurs if training data is scarce. Before being connected to the fully-connected neural network, the images need to be size normalized and centered in input fields. CNNs force the extraction of certain local features rather than global features which are obtained by hand-crafted feature extractors. LeCunn et al. [46] have worked in digit recognition and have received tremendous success on digit recognition.

Deep Learning research stopped even after all these breakthroughs because the computers took a lot of time to train the large neural nets and at the same time a lot of image data was also not available. Researchers thought that it is better to go ahead with hand-crafted feature extractors which were giving better results at that time and took less time for computation. In 2006, Geoffrey Hinton and Ruslan Salakhuditnov worked on reducing the dimension of the data with neural networks in thier paper [47]. Since then a lot of work has been done as computers have become powerful with the advent of modern parallel processing algorithms. One of the major breakthroughs came in 2012, when Alex Krizhevsky [48] build a huge neural network by training 15 million images from Imagenet [49] Database and then using Deep CNN they got one of the best result in the ImageNet competition for Image recognition and got a result which was nearly 11 p.c. better than the second best approach which was done with SIFT + Fisher Vectors [50]. Since

then in the last 4 years quite a good amount of work has been done in this field. Several deep learning frameworks have been designed by researchers for researchers to move the work ahead - Some of the famous Frameworks being Caffe [18] by University of California, Berkeley, Theano [19] by University de Montreal, TensorFlow [22] by Google, Torch [20] and many others.

In our project we have used the Caffe Deep Learning Framework [18] for our purposes. The reason we choose Caffe is being described below:

Caffe provides multimedia scientists and practitioners with a clean and modifiable framework for state of the art deep learning algorithms. It has a big collection of reference CNN models, it is licensed with BSD and is written in C++ and Python. Caffe can process upto 40 million images a day on a single NVIDIA K40. Caffe is maintained by Berkeley Vision and Learning Center(BVLC). Caffe makes it easy for users to build CNNs in their .prototxt file and also has several functions to draw networks and optimize them. It provides Pre-Trained models which is not provided by many of its competitors. Caffe stores and communicates data in 4-arrays called blobs for faster processing. Blobs provide a unified memory interface, holding batches of images , parameters or parameters updates. Blobs conceal the mental and mental overhead of mixed CPU/GPU operation by synchronizing from the CPU host to the CPU device as needed.

A key problem in multimedia data analysis is discovery of effective representations for sensory inputsimages, sound- waves, haptics, etc. While performance of conventional, handcrafted features has plateaued in recent years, new developments in deep compositional architectures have kept performance levels rising [48]. Deep models have outperformed hand-engineered feature representations in many domains, and made learning possible in domains where engineered features were

lacking entirely. We are particularly motivated by large-scale visual recognition, where a specific type of deep architecture has achieved a commanding lead on the state-of-the-art. These Con-volutional Neural Networks, or CNNs, are discriminatively trained via back-propagation through layers of convolutional filters and other operations such as rectification and pooling. Following the early success of digit classification in the 90s, these models have recently surpassed all known methods for large-scale visual recognition, and have been adopted by industry heavyweights such as Google, Facebook, and Baidu for image understanding and search.

While deep neural networks have attracted enthusiastic interest within computer vision and beyond, replication of published results can involve months of work by a researcher or engineer. Sometimes researchers deem it worthwhile to release trained models along with the paper advertising their performance. But trained models alone are not sufficient for rapid research progress and emerging commercial applications, and few toolboxes offer truly off-the-shelf deployment of state-of-the-art models and those that do are often not computationally efficient and thus unsuitable for commercial deployment.

Caffe has several advantages over its peers. Caffe provides a complete toolkit for training, testing, finetuning, and deploying models, with well-documented examples for all of these tasks. As such, its an ideal starting point for researchers and other developers looking to jump into state-of-the-art machine learning. At the same time, its likely the fastest available implementation of these algorithms, making it immediately useful for industrial deployment.

Some of the main features of Caffe are:

Modularity: The software is designed from the beginning to be as modular as

possible, allowing easy extension to new data formats, network layers, and loss functions. Lots of layers and loss functions are already implemented, and plentiful examples show how these are composed into trainable recognition systems for various tasks.

Separation of representation and implementation: Caffe model definitions are written as config files using the Protocol Buffer language. Caffe supports network architectures in the form of arbitrary directed acyclic graphs. Upon instantiation, Caffe reserves exactly as much memory as needed for the network, and abstracts from its underlying location in host or GPU. Switching between a CPU and GPU implementation is exactly one function call.

Test coverage: Every single module in Caffe has a test, and no new code is accepted into the project without corresponding tests. This allows rapid improvements and refactoring of the codebase, and imparts a welcome feeling of peacefulness to the researchers using the code.

Python and MATLAB bindings: For rapid prototyping and interfacing with existing research code, Caffe provides Python and MATLAB bindings. Both languages may be used to construct networks and classify inputs. The Python bindings also expose the solver module for easy prototyping of new training procedures.

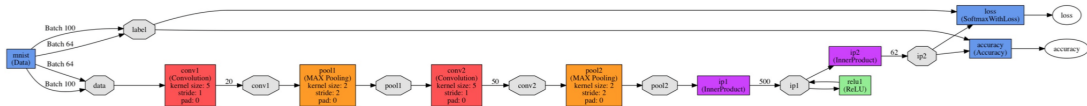


Figure 5.2. LeNet Network Diagram

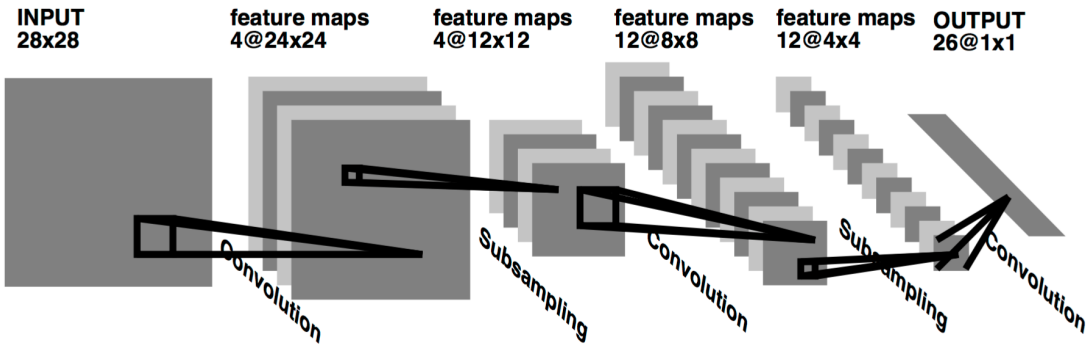


Figure 5.3. Typical CNN Network

5.2 Convolutional Neural Networks

Convolutional Neural Networks [45] combine different architectural ideas to ensure shift and distortion invariances. In the Figure 5.3 below it can be seen that the input plane receives images that are approximately size-normalized and centered. Each unit of a layer receives input from units which are located locally in the previous layer. With local fields, it becomes easier for the neurons to extract visual features such as oriented edges, corners etc, these features are then combined by the higher layer called feature maps. It is being stated that distortion or shift in inputs causes the position of the salient features to vary.

At each position, different types of units in different feature maps compute different types of features. A convolution layer is usually composed of several feature maps and as a matter of fact multiple features can be extracted at each location. The hidden layer in Figure 5.3 has 4 feature maps with 5 by 5 receptive fields.

Shifting the input of a convolution layer will shift the output. After detecting a feature, its location becomes less important as long as its relative position to other features is preserved. Thus, each convolution layer is followed by an additional layer while is called the pooling layer and it performs the subsampling and local averaging, thereby reducing the resolution of the feature map which reduces the effect to shifts and distortions. The second layer performs a 2 X 2 averaging and subsampling, followed by a trainable coefficient, a trainable bias , and a bias. The trainable coefficient and bias controls the effect of non-linearity. Then alternating layers of subsampling and convolutions are created successively where at each layer the number of feature maps are increased but the spatial resolution is decreased. The feature maps are then connected to form a fully-connected layer which is being fed into the softmax regression layer for classification purposes. All the weights are learned in the respective layers with back-propagation.

In recent times, Convolutional Neural Networks(CNNs) have almost been used in all applications ranging from the popular ImageNet Large Scale Visual Recognition Challenge(ILSVRC) to various Recognition algorithms. It has taken the computer vision society by storm, improving the state of the art in many applications. Tremendous results have been obtained in tremendous large scale databases in recent times.

ReLU Non-Linearity - In CNNs, the standard way to model a neuron's output f as a function of its input x is with $f(x) = \tanh(x)$ or $f(x) = (1+e^{-x})^{-1}$. The training time with gradient descent algorithm is much slower due to saturation and nonlinearities thus a new concept can be applied here with non saturating neurons with nonlinearities where $f(x) = \max(0,x)$. These nuerons are known as

Rectified Linear Units(ReLUs). CNNs with ReLUs train much faster than their corresponding tanh units. The performance of the neurons also does not decrease as proven with experiments by Hinton and Nair [51].

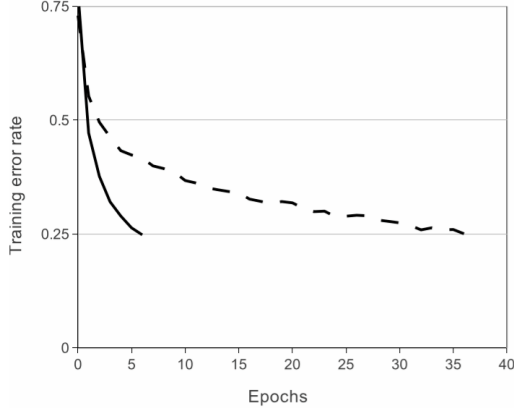


Figure 5.4. Performance of a 4-layer ReLU CNN

Figure 5.4 [48] shows the number of iterations required to reach 25 % training error on the CIFAR-10 dataset for a four layer convolution network. Thus it can be shown that faster learning has a great influence on the performance of large models which are trained on large datasets.

Another important concept to reduce test errors is the dropout technique. It seems to be too expensive for the big CNNs to train, which take several days to complete even on GPUs. The dropout technique consists of setting to zero the output of each hidden neuron with 50%. probability, the dropped out neurons do not contribute to the forward pass and also do not participate in back-propagation approach. So every time, the neural network samples a different architecture but all the architecture share weights. This technique reduces the complex co-adaptations of neurons since a neuron cannot rely on the presence of particular other neurons. It is, therefore, forced to learn more robust features that are useful in conjunction

with many different random subsets of the other neurons. At test time, we use all the neurons but multiply their outputs by 0.5, which is a reasonable approximation to taking the geometric mean of the predictive distributions produced by the exponentially-many dropout networks.

Dropout [52] is mostly applied to the Fully-connected layer in a CNN. Dropout helps to prevent overfitting in a neural network and thus is an extremely useful concept.

Chapter 6

Conclusion

In this project we have studied two scale and rotation invariant feature detectors and their application to ear recognition. Although both the SIFT and the SURF are invariant under scale and rotation changes, their performance decreases under certain conditions. The SIFT detector is more stable than the SURF detector under rotation changes. It is also found that the SIFT algorithm performs better for image decreasing, in contrast, the SURF algorithm performs better for image increasing. False matches have always caused problem for researchers in this field and it hinders the performance of the systems, thus Robust and Fast algorithm has been implemented to remove potential false matches and get better results. Experimental evaluations have demonstrated the effectiveness of the proposed techniques in ear recognition. For future work, an ear dataset consisting of thousands to millions of images must be created and preprocessed for better performances. Work must be done with the help of deep learning algorithms, which must be able to extract features automatically from less training data and as a matter of fact it would make it easier to train on CPUs and also give better performances.

Deep Learning models can be used for various purposes and thus the models must be applied to other biometric datasets to compare their performances. As of now, deep learning has mostly been applied to face recognition algorithms and has received tremendous success, thus work must be done on other sets of biometrics like iris, fingerprint, palm and others for better performances.

Bibliography

- [1] A. Pflug and C. Busch, “Ear biometrics: a survey of detection, feature extraction and recognition methods,” *Biometrics, IET*, vol. 1, no. 2, pp. 114–129, 2012.
- [2] C.-C. Chang and C.-J. Lin, “Libsvm: a library for support vector machines,” *ACM Transactions on Intelligent Systems and Technology (TIST)*, vol. 2, no. 3, p. 27, 2011.
- [3] A. Abaza, A. Ross, C. Hebert, M. A. F. Harrison, and M. S. Nixon, “A survey on ear biometrics,” *ACM computing surveys (CSUR)*, vol. 45, no. 2, p. 22, 2013.
- [4] A. Tariq and M. U. Akram, “Personal identification using ear recognition,” *TELKOMNIKA (Telecommunication Computing Electronics and Control)*, vol. 10, no. 2, pp. 321–326, 2012.
- [5] U. Park, S. Pankanti, and A. Jain, “Fingerprint verification using sift features,” in *SPIE Defense and Security Symposium*, pp. 69440K–69440K, International Society for Optics and Photonics, 2008.
- [6] A. Lannarelli, “Ear identification. forensic identification series,” 1989.

- [7] M. Burge and W. Burger, “Ear biometrics,” in *Biometrics*, pp. 273–285, Springer, 1996.
- [8] R. Purkait and P. Singh, “A test of individuality of human external ear pattern: Its application in the field of personal identification,” *Forensic science international*, vol. 178, no. 2, pp. 112–118, 2008.
- [9] D. G. Lowe, “Object recognition from local scale-invariant features,” in *Computer vision, 1999. The proceedings of the seventh IEEE international conference on*, vol. 2, pp. 1150–1157, Ieee, 1999.
- [10] D. G. Lowe, “Distinctive image features from scale-invariant keypoints,” *International journal of computer vision*, vol. 60, no. 2, pp. 91–110, 2004.
- [11] H. Bay, T. Tuytelaars, and L. Van Gool, “Surf: Speeded up robust features,” in *Computer vision–ECCV 2006*, pp. 404–417, Springer, 2006.
- [12] S. Sarkar, J. Liu, and G. Wang, “Biometric analysis of human ear matching using scale and rotation invariant feature detectors,” in *Image Analysis and Recognition - 12th International Conference, ICIAR2015, Niagara Falls, ON, Canada, July 22-24, 2015, Proceedings*, pp. 186–193, 2015.
- [13] J. Canny, “A computational approach to edge detection,” *Pattern Analysis and Machine Intelligence, IEEE Transactions on*, no. 6, pp. 679–698, 1986.
- [14] C. Harris and M. Stephens, “A combined corner and edge detector.,” in *Alvey vision conference*, vol. 15, p. 50, Citeseer, 1988.
- [15] D. J. Hurley, M. S. Nixon, and J. N. Carter, “Automatic ear recognition by force field transformations,” in *Visual Biometrics (Ref. No. 2000/018), IEE Colloquium on*, pp. 7–1, IET, 2000.

- [16] Z. Mu, L. Yuan, Z. Xu, D. Xi, and S. Qi, “Shape and structural feature based ear recognition,” in *Advances in biometric person authentication*, pp. 663–670, Springer, 2004.
- [17] S. A. Daramola and D. Oluwaninyo, “Automatic ear recognition system using back propagation neural network.,” *image*, vol. 9, p. 10, 2011.
- [18] Y. Jia, E. Shelhamer, J. Donahue, S. Karayev, J. Long, R. Girshick, S. Guadarrama, and T. Darrell, “Caffe: Convolutional architecture for fast feature embedding,” in *Proceedings of the ACM International Conference on Multimedia*, pp. 675–678, ACM, 2014.
- [19] J. Bergstra, O. Breuleux, F. Bastien, P. Lamblin, R. Pascanu, G. Desjardins, J. Turian, D. Warde-Farley, and Y. Bengio, “Theano: a cpu and gpu math expression compiler,” in *Proceedings of the Python for scientific computing conference (SciPy)*, vol. 4, p. 3, Austin, TX, 2010.
- [20] R. Collobert, S. Bengio, and J. Mariéthoz, “Torch: a modular machine learning software library,” tech. rep., IDIAP, 2002.
- [21] N. Whitehead and A. Fit-Florea, “Precision & performance: Floating point and ieee 754 compliance for nvidia gpus,” *rn (A + B)*, vol. 21, pp. 1–1874919424, 2011.
- [22] M. Abadi, A. Agarwal, P. Barham, E. Brevdo, Z. Chen, C. Citro, G. S. Corrado, A. Davis, J. Dean, M. Devin, *et al.*, “Tensorflow: Large-scale machine learning on heterogeneous distributed systems,” *arXiv preprint arXiv:1603.04467*, 2016.
- [23] I. Jolliffe, *Principal component analysis*. Wiley Online Library, 2002.

- [24] R. G. Cinbis, J. Verbeek, and C. Schmid, “Unsupervised metric learning for face identification in tv video,” in *Computer Vision (ICCV), 2011 IEEE International Conference on*, pp. 1559–1566, IEEE, 2011.
- [25] C. Lu and X. Tang, “Surpassing human-level face verification performance on lfw with gaussianface,” *arXiv preprint arXiv:1404.3840*, 2014.
- [26] M. Pietikäinen, “Local binary patterns,” *Scholarpedia*, vol. 5, no. 3, p. 9775, 2010.
- [27] N. Dalal and B. Triggs, “Histograms of oriented gradients for human detection,” in *Computer Vision and Pattern Recognition, 2005. CVPR 2005. IEEE Computer Society Conference on*, vol. 1, pp. 886–893, IEEE, 2005.
- [28] F. Perronnin, J. Sánchez, and T. Mensink, “Improving the fisher kernel for large-scale image classification,” in *Computer Vision–ECCV 2010*, pp. 143–156, Springer, 2010.
- [29] O. M. Parkhi, A. Vedaldi, and A. Zisserman, “Deep face recognition,” *Proceedings of the British Machine Vision*, vol. 1, no. 3, p. 6, 2015.
- [30] Y. Taigman, M. Yang, M. Ranzato, and L. Wolf, “Deepface: Closing the gap to human-level performance in face verification,” in *Proceedings of the IEEE Conference on Computer Vision and Pattern Recognition*, pp. 1701–1708, 2014.
- [31] P. Scovanner, S. Ali, and M. Shah, “A 3-dimensional sift descriptor and its application to action recognition,” in *Proceedings of the 15th international conference on Multimedia*, pp. 357–360, ACM, 2007.

- [32] F. Alonso-Fernandez, P. Tome-Gonzalez, V. Ruiz-Albacete, and J. Ortega-Garcia, “Iris recognition based on sift features,” in *Biometrics, Identity and Security (BIdS), 2009 International Conference on*, pp. 1–8, IEEE, 2009.
- [33] M. A. Fischler and R. C. Bolles, “Random sample consensus: a paradigm for model fitting with applications to image analysis and automated cartography,” *Communications of the ACM*, vol. 24, no. 6, pp. 381–395, 1981.
- [34] A. Hast, J. Nysjö, and A. Marchetti, “Optimal ransac-towards a repeatable algorithm for finding the optimal set,” 2013.
- [35] M. Zhang, G. Wang, H. Chao, and F. Wu, *Image Analysis and Recognition: 12th International Conference, ICIAR 2015, Niagara Falls, ON, Canada, July 22-24, 2015, Proceedings*, ch. Fast and Robust Algorithm for Fundamental Matrix Estimation, pp. 316–322. Cham: Springer International Publishing, 2015.
- [36] C. Cortes and V. Vapnik, “Support-vector networks,” *Machine learning*, vol. 20, no. 3, pp. 273–297, 1995.
- [37] K.-B. Duan and S. S. Keerthi, “Which is the best multiclass svm method? an empirical study,” in *Multiple classifier systems*, pp. 278–285, Springer, 2005.
- [38] L. M. E. Gonzalez, L. Alvarez, “Ami ear database, centro de i+d de tecnologias de la imagen,”
- [39] A. Kumar and C. Wu, “Automated human identification using ear imaging,” *Pattern Recognition*, vol. 45, no. 3, pp. 956–968, 2012.

- [40] S. Ansari and P. Gupta, “Localization of ear using outer helix curve of the ear,” in *Computing: Theory and Applications, 2007. ICCTA’07. International Conference on*, pp. 688–692, IEEE, 2007.
- [41] H. Chen and B. Bhanu, “Human ear detection from side face range images,” in *Pattern Recognition, 2004. ICPR 2004. Proceedings of the 17th International Conference on*, vol. 3, pp. 574–577, IEEE, 2004.
- [42] P. Yan and K. W. Bowyer, “Biometric recognition using 3d ear shape,” *Pattern Analysis and Machine Intelligence, IEEE Transactions on*, vol. 29, no. 8, pp. 1297–1308, 2007.
- [43] S.-C. Wang, “Artificial neural network,” in *Interdisciplinary Computing in Java Programming*, pp. 81–100, Springer, 2003.
- [44] Y. Le Cun, D. Touresky, G. Hinton, and T. Sejnowski, “A theoretical framework for back-propagation,” in *The Connectionist Models Summer School*, vol. 1, pp. 21–28, 1988.
- [45] Y. LeCun and Y. Bengio, “Convolutional networks for images, speech, and time series,” *The handbook of brain theory and neural networks*, vol. 3361, no. 10, p. 1995, 1995.
- [46] Y. LeCun, L. Bottou, Y. Bengio, and P. Haffner, “Gradient-based learning applied to document recognition,” *Proceedings of the IEEE*, vol. 86, no. 11, pp. 2278–2324, 1998.
- [47] R. Salakhutdinov and G. E. Hinton, “Deep boltzmann machines,” in *International conference on artificial intelligence and statistics*, pp. 448–455, 2009.

- [48] A. Krizhevsky, I. Sutskever, and G. E. Hinton, “Imagenet classification with deep convolutional neural networks,” in *Advances in neural information processing systems*, pp. 1097–1105, 2012.
- [49] J. Deng, W. Dong, R. Socher, L.-J. Li, K. Li, and L. Fei-Fei, “Imagenet: A large-scale hierarchical image database,” in *Computer Vision and Pattern Recognition, 2009. CVPR 2009. IEEE Conference on*, pp. 248–255, IEEE, 2009.
- [50] A. Berg, J. Deng, and L. Fei-Fei, “Large scale visual recognition challenge 2010,” 2010.
- [51] V. Nair and G. E. Hinton, “Rectified linear units improve restricted boltzmann machines,” in *Proceedings of the 27th International Conference on Machine Learning (ICML-10)*, pp. 807–814, 2010.
- [52] N. Srivastava, G. Hinton, A. Krizhevsky, I. Sutskever, and R. Salakhutdinov, “Dropout: A simple way to prevent neural networks from overfitting,” *The Journal of Machine Learning Research*, vol. 15, no. 1, pp. 1929–1958, 2014.

Chapter 7

Appendix

1. Code for Robust Fundamental Matrix

```
function [F, inliers] =RobustFundamentalMatrix(x1, x2)
numpts=size(x1, 2);
[Fi, e1i, e2i]=fundmatrix(x1, x2);
Pai=eye(3, 4); Pbi = vgg_P_from_F(Fi);
Xe=zeros(4, numpts);
err=zeros(1, numpts);
et=err;
for i=1:numpts
    Xe(:, i)=optimalTriangulation(x1(:, i), x2(:, i), Pai, Pbi, Fi, e1i, e2i);
    err(i)=sqrt(norm(pflat(Pai*Xe(:, i))-x1(:, i))^2+
                 norm(pflat(Pbi*Xe(:, i))-x2(:, i))^2);
    et(i)=sum(pflat(Pai*Xe(:, i))-x1(:, i))+
           sum(pflat(Pbi*Xe(:, i))-x2(:, i));
end
```

```

end

m=median( abs( err ) );
sigma=1.4826*(1+5/(numpts-8))*m;
index=find( abs( err )<3*sigma );
[F, e1 , e2]=fundmatrix( x1( : , index ) , x2( : , index ) );
Pa=eye( 3 , 4 );Pb = vgg_P_from_F(F);
for i=1:numpts
    Xe( : , i)=optimalTriangulation( x1( : , i ) , x2( : , i ) , Pa , Pb , F , e1 , e2 );
    err( i)=sqrt( norm( pflat( Pa*Xe( : , i ))-x1( : , i ))^2+
        norm( pflat( Pb*Xe( : , i ))-x2( : , i ))^2 );
    et( i)=sum( pflat( Pai*Xe( : , i ))-x1( : , i ))+
        sum( pflat( Pbi*Xe( : , i ))-x2( : , i ) );
end

m=median( abs( err ) );
sigma=1.4826*(1+5/(numpts-8))*m;
index=find( abs( err )<3*sigma );
F=fundmatrix( x1( : , index ) , x2( : , index ) );
inliers=index ;

```

2. Code for Optimal Triangulation

```

function X = optimalTriangulation( x1 , x2 , P1 , P2 , F , e1 , e2 )
% [ X, r ] = optimalTriangulation( x1 , x2 , P1 , P2 , F , e1 , e2 )
%     Optimal solution for MLE, using method proposed by Hartley(P315).
%     Finding optimal solution by finding real solutions of a polynomial
%     equation of degree 6.

```

%

if any(size(x1) ~= size(x2))

error('size(x1) ~= size(x2)');

end

if size(x1,1)==2 % convert x1,x2 to form of (x,y,1)

x1=[x1;1];

x2=[x2;1];

else

x1(1)=x1(1)./x1(3);x1(2)=x1(2)./x1(3);x1(3)=1;

x2(1)=x2(1)./x2(3);x2(2)=x2(2)./x2(3);x2(3)=1;

end

T1=[1 0 -x1(1);0 1 -x1(2);0 0 1]; T1_inv=[1 0 x1(1);0 1 x1(2);0 0 1];

T2=[1 0 -x2(1);0 1 -x2(2);0 0 1]; T2_inv=[1 0 x2(1);0 1 x2(2);0 0 1];

F=T2_inv.*F*T1_inv;

%x1=[0;0;1];%T1*x1;

%x2=[0;0;1];%T2*x2;

e1=T1*e1; e1=e1/norm(e1(1:2));

e2=T2*e2; e2=e2/norm(e2(1:2));

R1=[e1(1) e1(2) 0;-e1(2) e1(1) 0;0 0 1];

R2=[e2(1) e2(2) 0;-e2(2) e2(1) 0;0 0 1];

%e1=[1;0;e1(3)];%R1*e1;

%e2=[1;0;e2(3)];%R2*e2;

```

F=R2*F*R1 . ' ;
f1=e1(3); f2=e2(3); a=F(2,2); b=F(2,3); c=F(3,2); d=F(3,3);
%F_=[f1*f2*d -f2*c -f2*d;-f1*b a b;-f1*d c d];
%F ./ F_
f1_2=f1^2; f1_4=f1_2^2; f2_2=f2^2;
k1=a^2+f2_2*c^2; k2=2*(a*b+f2_2*c*d); k3=b^2+f2_2*d^2;
k=a*d-b*c; k4=a*c; k5=b*c+a*d; k6=b*d;
c6=-f1_4*k4;
c5=k1^2 - f1_4*k5;
c4=2*k1*k2 - 2*f1_2*k4 - f1_4*k6;
c3=k2^2 + 2*k1*k3 - 2*f1_2*k5;
c2=2*k2*k3 - k*k4 - 2*f1_2*k6;
c1=k3^2 - k*k5;
c0=- k*k6;
% Threshold to set some very samll cis to 0.
p=[c6 c5 c4 c3 c2 c1 c0];
Mci=max( abs(p));
for i=1:6
    if abs(p(i))<Mci*1e-25 % threshold ratio is chosen to be 1e-20
        p(i)=0;
    end
end
if sum(isnan(p))^=0 || sum(isinf(p))^=0

```

```

X=zeros(4,1); return
end
rs=real(roots(p));
nrs=size(rs,1);% number of roots.
s=zeros(nrs+1,1);
for i=1:nrs
    t=rs(i);
    t2=t^2;
    k1_=(a*t+b)^2;
    k2_=(c*t+d)^2;
    s(i)=t2/(1+f1_-2*t2)+k2_/(k1_-+f2_-2*k2_);
end
s(nrs+1)=1/f1_-2+c^2/(a^2+f2_-2*c^2);
[m I]=min(s);
if I==nrs+1
    l1=[f1;0;-1];
    l2=[-c*f2;a;c];
else
    t=rs(I);
    l1=[t*f1;1;-t];
    l2=[-f2*(c*t+d);a*t+b;c*t+d];
end
x1_=[-l1(1)*l1(3); -l1(2)*l1(3); l1(1)^2+l1(2)^2];
x2_=[-l2(1)*l2(3); -l2(2)*l2(3); l2(1)^2+l2(2)^2];
%r=sqrt((x1_(1)^2+x1_(2)^2)/x1_(3)^2+(x2_(1)^2+x2_(2)^2)/x2_(3)^2);

```

```

% residual
%r=sqrt (m);
x1_=T1_inv*R1.' * x1_;
x2_=T2_inv*R2.' * x2_;

Ax=zeros (4 ,4);
Ax(1 ,:) = x1_(1)*P1(3 ,:) - x1_(3)*P1(1 ,:);
Ax(2 ,:) = x1_(2)*P1(3 ,:) - x1_(3)*P1(2 ,:);
Ax(3 ,:) = x2_(1)*P2(3 ,:) - x2_(3)*P2(1 ,:);
Ax(4 ,:) = x2_(2)*P2(3 ,:) - x2_(3)*P2(2 ,:);
[u s v]=svd (Ax);
X=v (: ,end );

end

```

3.Basic Code for SIFT Matching

```

[image1 ,descripts ,locs]=sift ('ear1.pgm');
% You cannot change the name of the locs , that is why, it is
being stored in
% loc1 for later use
locs1=locs;%loc1 is locs for first first image,same with loc2
and descripts1 and descripts 2.
descripts1=descripts;
[image2 ,descripts ,locs]=sift ('ear1.pgm');
locs2=locs ;

```

```

descripts2=descripts;
[num, matches] = match(image1, descripts1, locs1, image2, descripts2, locs2);
if num<5
    fprintf('Match Failed')
    title('Match Failed')
    return
end

x1=[loc1(matches(1,:),1:2),ones(size(matches,2),1)]';
x2=[loc2(matches(2,:),1:2),ones(size(matches,2),1)]';
[F,inliers]=RobustFundamentalMatrix(x1,x2);
threshold=0.7;
if length(inliers)/size(matches,2)>threshold
    result=1;
    fprintf('Match');
    title('Match')
else
    result=0;
    fprintf('Failed');
    title('Failed');
end

```

4.Basic Code for SURF Feature extraction

```

I1 = imread('ear1.pgm');
I2 = imread('ear2.pgm');
points1 = detectSURFFeatures(I1);

```

```
points2 = detectSURFFeatures(I2);  
[f1, vpts1] = extractFeatures(I1, points1);  
[f2, vpts2] = extractFeatures(I2, points2);  
index_pairs = matchFeatures(f1, f2) ;  
matched_pts1 = vpts1(index_pairs(:, 1));  
matched_pts2 = vpts2(index_pairs(:, 2));  
figure, showMatchedFeatures(I1, I2, matched_pts1, matched_pts2);  
title('Putative point matches');  
legend('matchedPts1', 'matchedPts2');
```